MATHEMATICAL SIMULATION OF A HORIZONTAL FLUE RING FURNACE

R.T. Bui, E. Dernedde*, A. Charette, T. Bourgeois

Université du Québec, Chicoutimi, P.Q., Canada G7H 2B1
*Alcan International Ltd., P.O.B. 1250, Arvida, Canada, G7S 4K8

A mathematical model is developed in which the horizontal flue ring furnace is treated as a continuous counterflow heat exchanger. The model integrates the equations of heat transfer between flue gas and solids along the entire length of the furnace, and the heat conduction equations within the solids (bricks, coke and anode). Infiltration and volatiles are treated by appropriate sub-models. Simulation runs are made which succeed in reproducing the operating conditions of the Arvida ring furnaces.

Introduction

A mathematical model for the horizontal flue ring furnace used in the baking of carbon anodes at the Arvida Works of Alcan Smelters and Chemicals Ltd., Arvida, Canada, has been developed for the purpose of analyzing the behavior and performance of the furnace in response to various parameter changes. Published literature on the modeling of the overall process in the horizontal flue ring furnace is scarce [1]. The purpose of this work is to develop a computer model not too cumbersome yet capable of taking into account the numerous aspects of the baking process, the most important of which being the air infiltration, the draft control, the release of volatiles and their burning.

The model

The model is based on the assumption that the furnace is a continuous counterflow heat and mass exchanger, where the gas flows in flues from right to left (Fig. 1), and the solids " flow " in pits from left to right. The gas flows at changing velocity determined by its mass, pressure and temperature. The solids " flow " at constant velocity equal to the length of one pit divided by fire-step time. This calls for a balance equation for the gas to wall exchange.
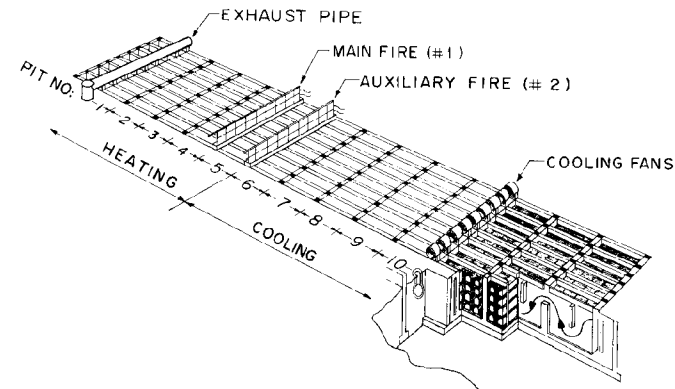

Fig. 1 A three-dimensional view of the ring furnace

This balance equation is written for a control volume extending from the top of the uppermost anode to the bottom of the lowermost anode, and from the centerline of a flue to the centerline of the adjacent pit, and of length δx along the furnace. This yields:

$$\dot{m}_g C_{pg} \frac{\partial T_g}{\partial x} + \alpha \frac{\partial \dot{m}_g}{\partial x} C_{pg} (T_g - 300) - 2h_T R(T_g - T_w) + \dot{m}_f H_f + \alpha\beta\dot{m}_v H_v = 0 \qquad (1)$$

$\dot{m}_g$ = gas mass flow in flue   [kg/s]

C_{pg} = specific heat of gas   [J/kg.K]

T_g = gas temperature [K]

300 = ambient air temperature [K]

h_T = total heat transfer coefficient between gas and wall
(convection and radiation) [W/m².K]

R = depth of pit [m]

T_W = wall temperature [K]

$\dot{m}_f$ = fuel injection per unit furnace length [kg/m.s]

$\dot{m}_v$ = volatiles (CH_4, H_2, tar separately) release rate
per unit furnace length [kg/m.s]

H_f, H_v = heat of reaction of fuel and of volatiles [J/kg]

α = binary variable, 1 for heating zone, 0 for cooling
zone

β = percent of volatile release that combusts.

The heat thus exchanged from the gas to the brick wall (in the heating section, or conversely in the cooling section), is then transferred through the three solids (brick, coke, anode) by conduction. This calls for a set of equations describing the two-dimensional heat conduction at different nodes inside and on the face and interface of the solids. These equations are of the type:

$$T_0^{t+\Delta t} = T_0^t + \frac{\Delta t}{\rho C_p} . [\frac{K_1}{\Delta z^2} (T_1^t - T_0^t) + \frac{K_3}{\Delta z^2} (T_3^t - T_0^t) + \frac{K_2}{\Delta y^2} (T_2^t - T_0^t) + \frac{K_4}{\Delta y^2}(T_4^t - T_0^t) \quad (2)$$

written for an internal node as represented in Fig. 2. The conductivities are taken as arithmetic means of the two values at the two nodes concerned.
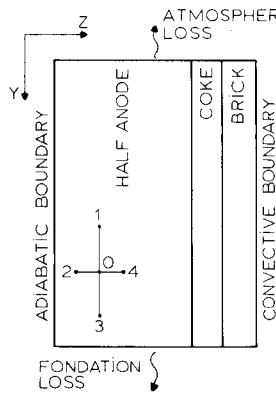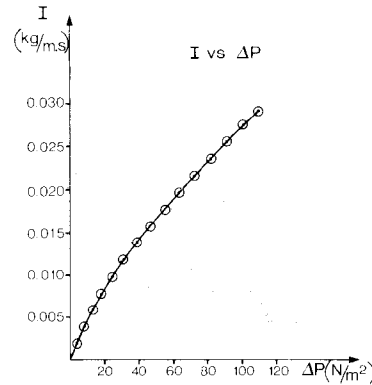

Fig. 2 The control volume

Fig. 3 Infiltration vs draft

For nodes on the convective boundary (brick wall), the K_4 term is replaced by a convection term. For nodes on the adiabatic boundary (anode centerline), the K_2 term simply vanishes. For nodes along the top boundary, the K_1 term is replaced by a term representing the heat loss to the atmosphere. For nodes along the bottom boundary, the K_3 term is replaced by a term representing the heat loss to the foundation. These loss terms are supplied by a separate calculation of losses performed on the furnace, then introduced into this model as a curve in order to avoid making the model unduly cumbersome.

Equation (1) together with the equations (2) constitute the main body of the model. Using appropriate boundary conditions, its solution yields the temperature of the flue gas and of the different solids at different locations, along the entire length of the furnace.

The solution is performed by Euler explicit method using finite differences. The criterion for choosing the solution method is speed of execution.

Infiltration and draft

Infiltration and draft are related. To obtain this relation, we proceed as follows. Starting with a set of experimental data on gas mass flow profile along the furnace $\dot{m}_g(x)$, and a set of experimental data on draft profile along the furnace $\Delta P(x)$ we differentiate to obtain the infiltration profile:

$$I(x) = - \frac{d\dot{m}_g(x)}{dx}$$

then plot $I(x)$ versus $\Delta P(x)$ to have the experimental curve:

$$I = f(\Delta P) \qquad (3)$$

which is then curve-fitted with a polynomial (Fig. 3). Thus knowledge of draft ΔP will give infiltration I. In order to determine ΔP, we write a momentum balance for the gas in a slice Δx of the flue, then use relation (3) and this momentum balance alternatively to calculate ΔP for each slice of the furnace in an iterative manner, all the while insuring that ΔP just behind the fires (pit No. 5) must pass through zero as required for good operation of the furnace.

The volatiles

As for volatiles, two problems must be tackled: volatile release from the anodes, and volatile burning. An approach to the former is presented here, while the latter requires trial-and-error to determine the percentage of volatiles actually combusted.

Laboratory analysis provides us with the percentage volatile release for each species of volatiles (methane, hydrogen and tar) in kg volatile per kg anode as function of anode temperature T_a. Multiplied by the mass of anodes per meter of furnace length, this yields the volatile release in kg volatile per meter of furnace. Such a curve $m_v(T_a)$ when differentiated gives $\partial m_v / \partial T_a$. On the other hand, starting from a typical anode temperature profile $T_a(t)$, we differentiate to obtain $\partial T_a / \partial t$, and a multiplication yields

$$\dot{m}_v = \frac{\partial m_v}{\partial T_a} \times \frac{\partial T_a}{\partial t} = \frac{\partial m_v}{\partial t} \qquad [\frac{kg\ vol}{m.h}]$$

The same operation is performed three times, for methane, hydrogen and tar respectively. Fig.4 presents the three resulting curves giving the release rate of each of three species of volatiles as function of anode temperature.

As for volatile burning, we assume that combustion occurs in the flue and not in the solids, and we adjust the parameter β so as to obtain the
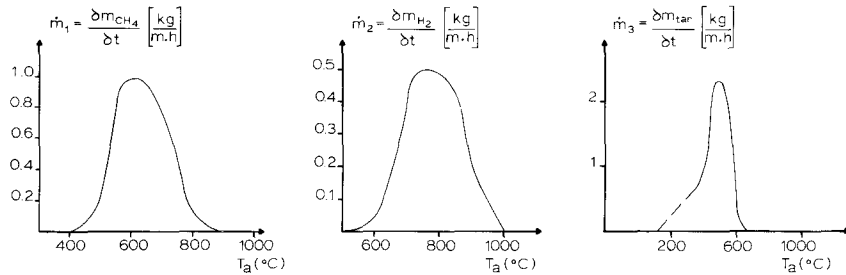
Fig. 4   Release rate of methane, hydrogen and tar
as function of anode temperature

right exhaust gas temperature which is $T_g(0) = 740$ K. At each point along
the furnace, it is also verified to see if gas temperature is high enough
to insure volatile combustion, knowing the ignition temperatures to be 848 K
for hydrogen, 903 K for methane and 695 K for tar, the latter being an ave-
rage. It turns out that this condition is always satisfied, gas temperatu-
res at the points concerned being consistently higher than the ignition tem-
peratures mentioned. As a result, it is found that volatile combustion is
spread from pit 1 to pit 4, and that $\beta = 0.78$, meaning that in total, 78
percent of the volatiles released actually combust.

Procedure for computation

First and foremost, we must bear in mind that the thermal properties
of the gas as well as of the three solids are variable. Thus in equations
(2), specific heats C_p and conductivities K vary from one solid to another
and also within the same solid as temperatures vary. In equation (1), h_T,
which is the sum of convection heat transfer coefficient and radiation heat
transfer coefficient, $h_T = h_c + h_r$, varies with gas flow, gas composition
and gas temperature. Also in equation (1), C_{pg} varies with gas temperature
and composition.

The above is to say that some preliminary calculation needs to be done
before we can enter the model itself. We proceed as follows:

1- The infiltration sub-model is solved first. Starting from an assu-
med profile of gas temperature and a known " target " value (gas flow at
entrance of cooling zone, or at burners, or at exhaust), we obtain the gas
flow profile $\dot{m}_g(x)$ and the draft profile $\Delta P(x)$ along the furnace.

2- Then, starting from $\dot{m}_g(x)$ thus obtained, calculate h_c using the
Dittus-Boelter correlation. Starting from an assumed value of $\dot{m}_f(x)$, cal-
culate h_r. Add the two to obtain h_T. Also, C_{pg} is calculated based on the
concentration of CO_2, H_2O, O_2 and N_2 at each slice along the furnace.

3- Input the values of h_T and C_{pg} thus found into the model itself in
order to solve equations (1) and (2) from one end of the furnace to the
other and obtain a new gas temperature profile $T_g(x)$ and solid temperature
profiles $T_w(x)$, $T_c(x)$, $T_a(x)$ where subscripts w, c, a are for wall, coke and
anode respectively. Since we start from one end and move toward the other,

this part of the computation is referred to as " shooting " . Although it
is not strictly necessary to do so, we used to start from left, using the
initial solid temperature 50°C and the exhaust gas temperature 467°C as boun-
dary values and in doing the " shooting " , we aim at the known values of
maximum gas temperature and maximum baking temperature. Air inlet tempera-
ture at the right end of furnace is also a useful control target. Shooting
is done by adjusting the fuel flow $\dot{m}_f(x)$ so as to reach the known targets.
Also, the value of β is adjusted the same way to find out the percentage of
volatiles burned.

4- Finally, compare the new $T_g(x)$ profile found in step 3 with the as-
sumed $T_g(x)$ profile used in step 1. If they differ, go back to step 1.
Otherwise, computation ends. Usually, no more than two such iterations are
needed.

The final product of this exercise is a temperature profile along x for
the gas and for each solid, and also a two-dimensional isothermal map at
each section along the furnace.

Results

Fig. 5 presents the temperature profiles along the furnace for the wall
and for the anodes, calculated and experimental. Temperature profiles for
the gas, the brickwork, the coke are also available from the model but are
not reproduced here, to avoid overloading the figure. Anode temperatures
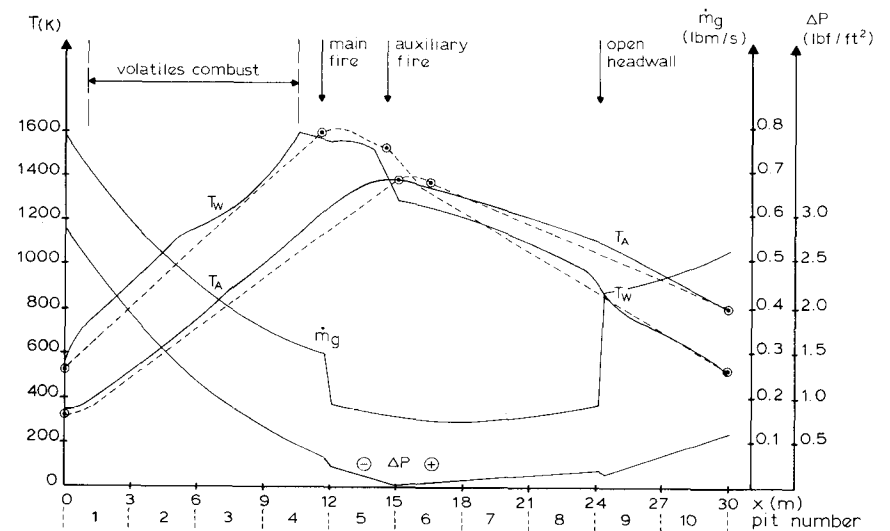are taken at the geometrical centre of the pit.

Fig. 5   Profiles for wall and anode temperatures along the furnace, cal-
culated versus experimental. Experimental data come from several
sets of measurments, important data points are encircled.

It can be seen that the calculated profiles compare reasonably well with the experimental ones. Note that the experimental data used for comparison in Fig. 5 come from more than one set of measurements but they are all consistent with one another.

Several simulations are now made, some of them are of a " theoretical " nature such as lengthening or shortening the heating and the cooling zones, while others reproduce the physical experimentations which have actually been performed on the Arvida furnaces in the recent past. The latter series includes simulation of the changing of baking temperature, the changing of cooling air flow, the reduction of infiltration by use of pit covers, the changing of fire-cycle time, and the injection of water into the flues. In all these tests, the calculated results agree with the measurements from fairly well to very well.

The last test, concerning water spray cooling, is presented here partly because the results of the experimental investigation by Holdner and Proulx are available to the readers [2]. We inject the same flow of water as used in the investigation i.e. 38 liters per hour per flue. The anode temperature profiles found are presented on Fig. 6 together with the experimental results by Holdner and Proulx. It can be seen that they are in very good agreement. Other elements of comparison (fuel flow, heat transfer coefficient, specific heat of gas) also agree although not mentioned on the figure. Notice that the simulation shows the changes in anode cooling rate the same way they have been measured experimentally. In particular, the anode temperature difference between air cooling and water spray cooling, experimentally found to be 140°, is given as 136° by the simulation.

Conclusion

It is believed that the model proposed is simple enough to be useful yet elaborate enough to be representative of the process, provided the necessary data be available so that appropriate calibration can be made. It constitutes a good tool for process evaluation as well as for process improvement.

References

[1] Keller F. and Disselhorst J.H.M. " Modern Anode Bake Furnace Developments " . Lightmetals 1981, pp. 611-621.

[2] Holdner D.N. and Proulx A.L. " Water Addition to the Cooling Sections of Horizontal Flue Ring Furnaces " . Lightmetals 1981, pp. 597-609.
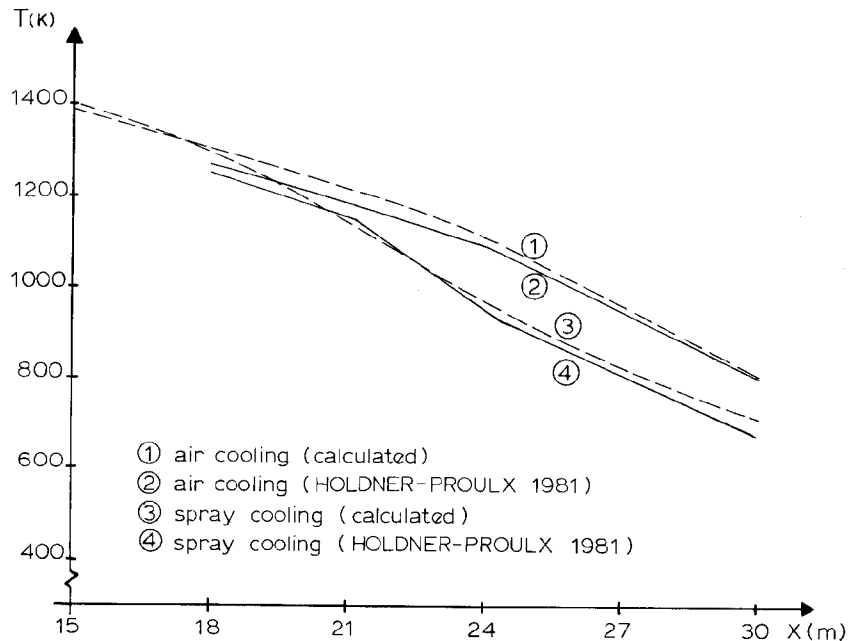

Fig. 6 Profiles for anode temperatures in the cooling zone, with air cooling and water spray cooling, calculated versus experimental. Experimental data comes from Holdner and Proulx's investigation.